Determination of aerodynamic force coefficients of octagonal lighting columns from wind tunnel experiments

Donatienne PORTUGAELS [*], Jérôme ANTHOINE [**], Domenico OLIVARI [***]
[*] Direction de Contrôle et des Réceptions techniques
Direction générale des Services techniques
Ministère wallon de l'Equipement et des Transports
Boulevard du Nord 8 – 5000 NAMUR
BELGIUM
http://www.met.wallonie.be
[**] von Karman Institute for Fluid Dynamics,
Chaussée de Waterloo 72 – 1640 Rhode-Saint-Genèse, Belgium
http://www.vki.ac.be
[***] AirSR, Bruxelles, Belgium & von Karman Institute, Rhode-Saint-Genèse, Belgium

Abstract: - The design of the lighting columns with octagonal cross-section, to be used along public roads, requires a precise knowledge of their aerodynamic force coefficients. The aerodynamic forces induced by the wind on octagonal cylindrical elements with different diameters, different edge curvature radii and different roughness's have been measured in a wind tunnel in order to determine the influence of these parameters on the aerodynamic force coefficients.

Key-Words: - Aerodynamic force coefficient, Drag, Lighting columns, Blockage effect, Wind tunnel, Roughness, Edge curvature radius.

1 Introduction

The present article aims to describe the investigation performed to determine the aerodynamic force coefficients of public lighting columns with octagonal cross-section. This experimental study was carried out at the von Karman Institute for Fluid Dynamics for the ministère wallon de l'Equipement et des Transports M.E.T. (Belgium) – Direction générale des Services techniques D.G.4 – Division de l'Electricité, de l'Electromécanique, de l'Informatique et des Télécommunications D.E.E.I.T.

1.1 Ministère wallon de l'Equipement et des Transports (M.E.T.)

Created in 1989, the ministère wallon de l'Equipement et des Transports (M.E.T.) has taken over, for the Walloon Region (south part of Belgium), the responsibilities of the former Belgian ministry of Public Works. Its mission consists in building, equipping, managing, developing and maintaining the following communication ways: 8636 km of roads (including 800 km of highways), 451 km of waterways (including harbors and hydraulic civil engineering structures), regional airports and the telecommunication network used by the ministry to diffuse in real time the information about the operability situation of all the infrastructures.

1.2 The von Karman Institute for Fluid Dynamics (VKI)

The von Karman Institute for Fluid Dynamics, founded in 1956, is an international non profit organization for post graduate education and research in fluid dynamics. Permanent staff of VKI is about 95 in total, spread over its 3 departments: Aeronautics and Aerospace, Environmental and Applied Fluid Dynamics, Turbomachinery and Propulsion. The research and training activities are carried out combining experimental (with a total of 43 wind tunnels and test rigs), theoretical and numerical approaches, and span over aeronautical and non-aeronautical flow applications of industrial interest.

1.3 Public lighting columns used in Belgium (Walloon Region)

The principal types of public lighting columns used in the Walloon Region are: straight columns, columns with arms and ornamental columns. The two first types present an octagonal cross-section with a linearly increasing diameter from the base to the top. The last ones are composed of a base made of one or several circular element(s) and an ornamental top. All of them are made of steel.

1.4 Objective of the research project

The aerodynamic behavior of circular cylinders is well known, including the effect of surface roughness on the drag coefficient. However, the lighting columns have an octagonal cross-section with rounded edges. When produced, the columns are galvanized to be protected against corrosion. After years, the protection is less efficient and corrosion is appearing. This corrosion is modifying the surface roughness of the columns. This is the reason why the objective of the present research was to investigate the effect of the rounded edge radius and of the surface roughness on the aerodynamic force coefficients of the octagonal lighting columns. Some tests were however performed considering circular cylinders to compare them to the literature and so validating all the results. A precise knowledge of the aerodynamic force coefficients is indeed the prerequisite for the design of the public lighting columns.

2 Previous studies

The literature related to the drag coefficient of octagonal cylinders, with influences of rounded edge radius and of surface roughness, is quite poor. On the other hand, the flow around a circular cylinder has been widely investigated, some articles dating from the beginning of the fluid dynamics studies. Different kinds of transitions can occur in the wake of the cylinder. The Reynolds number characterizes the flow regime and thus the drag induced by the wind on the cylinder. The evolution of the drag coefficient with the Reynolds number for a circular cylinder appears in many references [1-17] and is given in Fig. 1.

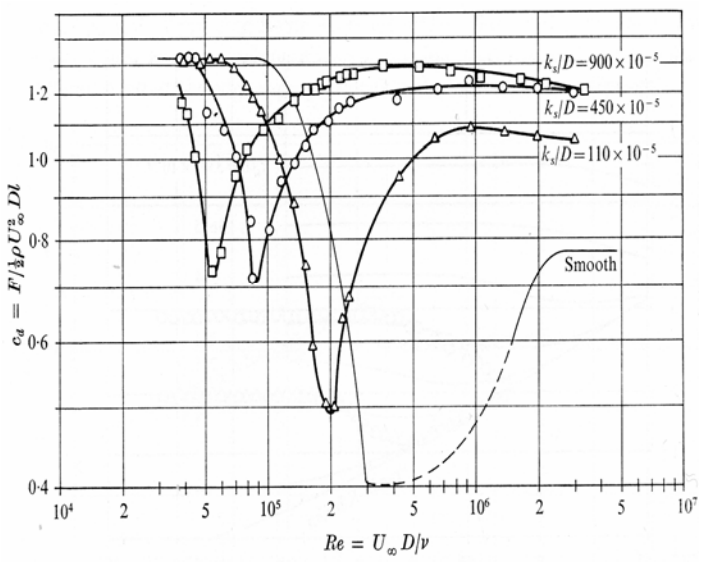

Fig. 1 – Drag coefficient evolution of circular cylinders with different surface roughness [11].

The critical regime appearing for Reynolds number around Re = 3 x 10^5 is associated with a strong decrease of drag coefficient. The drag evolutions in the critical regime vary significantly from one author to another, sometimes in a ratio of 3 for the same Reynolds number, as reported in the literature [7,17]. This could be explained by the high sensitivity of the boundary layer transition to external parameters, such as the cylinder roughness, the turbulence intensity of the upstream flow, the blockage ratio (ratio between the model and the wind tunnel cross-section areas), the aspect ratio of the model and the geometry of the end plates.

On both side of this critical regime, the drag coefficient is characterized by two constant values. In practice, these two values correspond to the most critical ranges of Reynolds numbers, in term of drag on the cylinder. Indeed, the critical regime being associated to a strong decrease of drag coefficient, the only regimes for which the drag force is important are the sub-critical and the early super-critical regimes. Later in the super-critical regime, both the Reynolds number and the drag coefficient are still higher but the wind velocity is out of the common practical range (< 200 km/h).

The effect of surface roughness on the drag coefficient has also been widely investigated [11-16] and is shown in Fig. 1. Below a critical relative roughness (k_s/D = Ra/d (later in the text) = 5 x 10^{-4}), the drag evolution is identical than for a smooth circular cylinder. Above that value, the Reynolds number associated to the critical point (minimum of drag coefficient) diminishes and the minimum drag coefficient increases.

The upstream turbulence level has a similar influence on the drag coefficient than the surface roughness by acting on the laminar-turbulent transition [18-20].

For an infinite cylinder with octagonal cross-section, the literature provides a drag coefficient of 1.4 [10,21]. However, this value has to be considered with care [22] since the literature is not indicating information on the conditions under which this value was obtained. For polygonal cylinders, the drag coefficient diminishes when the number of sides increases [22-26]. The effect of the surface roughness on the drag coefficient of octagonal cylinders is not reported in the literature.

Only a few previous studies exist on the influence of the rounded edge radius. The drag coefficient is reduced when rounding the cylinder edges. For small relative edge radius (sharp edge), the drag coefficient is independent of the Reynolds number. When the relative edge radius increases, the drag coefficient diminishes and the transition appears for smaller Reynolds number. However, the conditions of the tests are not enough documented for being used in the design of the public lighting columns, which reinforce the necessity of the present investigation.

3 Wind tunnel experiments

One solution to investigate the lighting columns consists to test scaled models simulating the entire column. This solution allows taking into account the conical shape of the real lighting columns. However, these scaled models do not allow to tackle the effect of the roughness, of the edge radius, … The other solution, followed here, consists in testing 2-D cylindrical models at full-scale.

3.1 The wind tunnel

The measurements have been performed in the free jet test section of the VKI low speed wind tunnel L-1A. The test section of 3 m diameter and 4,5 m length is adapted with a rectangular insert with solid side, top and bottom walls that is used for tests of 2-D models. This insert corresponds to a closed test section, whose dimensions are 2,372 m for the height, 1,294 m for the width and 4,25 m for the length in the flow direction.

The flow velocity can vary continuously from 2 to 50 m/s. The wind tunnel flow is provided by two contra-rotating propellers operated by a motor of 580 kW. The contraction ratio is 4 with a typical turbulence level of 0.3% (Fig. 2).

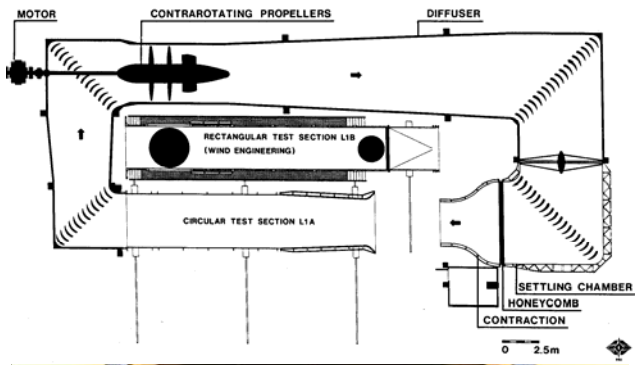

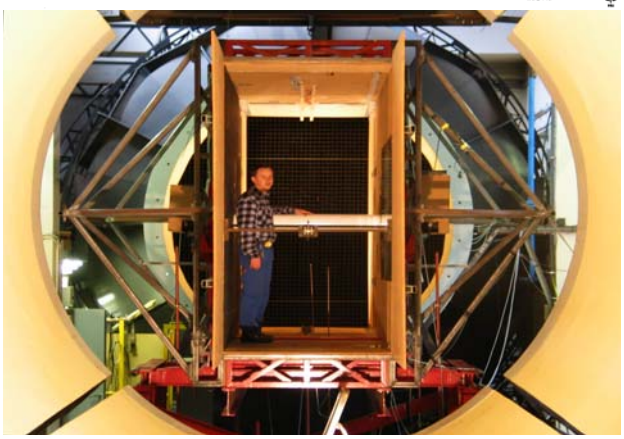

Fig. 2 – The wind tunnel and the rectangular insert for test of 2-D models

3.2 The instrumentation

The free stream reference flow velocity U is measured using a Pitot tube connected to a pressure transducer.

The drag force is measured using two strain gauges balances connected to both extremities of the cylinder. The instantaneous drag results are recorded on a PC, before being averaged. It was checked that the mean value is independent of the number of acquisition points.

3.3 The models

The evolution of the drag coefficient should be measured for Reynolds numbers ranging from 8×10^4 to 1.3×10^6 to cover the transition. This allows simulating the common practical range of wind velocity (from 10 km/h to 180 km/h) corresponding to the sub-critical, the critical and the super-critical flow regimes.

To cover the Reynolds number range, cylinders of different diameters are used, up to a diameter of 400 mm. In such conditions, the blockage effect cannot be neglected and corrections should be applied as indicated below.

In total, 27 models, made in wood, have been tested, among which 6 present a circular cross-section and 21 have an octagonal cross-section with different edge radii. The models differ also from their diameter, ranging from 60 mm to 400 mm, and from their surface roughness. The extreme diameters correspond to the base and top diameters of real lighting columns; the other diameters are tested to determine the influence of this parameter on the drag coefficient.

The different edge radii have also been selected to provide a good knowledge of its effect on the drag. Absolute values are equal to 0, 5, 10, 15, 20, 25 and 40 mm. The usual edge radius for the real columns is between 6 and 10 mm. Four surface roughnesses are considered. They were defined from absolute roughness measured on existing lighting columns. Table 1 provides the type of roughness, the desired roughness value (from measurements on real columns) and the achieved roughness value obtained by covering the models with different glued roughness papers. All the details concerning the models are reported in Table 2.

Table 1 – Roughness values tested in wind tunnel

Nr.	Type of roughness	Desired Ra [µm]	Achieved Ra [µm]
A	Smooth	≤ 1	0.21
B	Galvanized	3	2.88
C	Rusted	20	23.88
D	Highly rugged	> 30	46.79

A comparison between a cut of a real column made of steel and a wood model with the same geometrical parameters has been made (see models 26 and 27). The drag coefficient evolutions are very similar (Fig. 3), which fully validated the use of wood models for the measurements in wind tunnel. The small difference is justified by the slight deviation in surface roughness.

Table 2 – Model definition

Nr.	Diameter, d [mm]	Edge radius, r [mm]	r / d	Rough-ness, Ra [µm]	Ra / d
1	60	10	0.17	0.21	$3.5 \cdot 10^{-6}$
2	60	10	0.17	2.88	$4.8 \cdot 10^{-5}$
3	60	10	0.17	23.88	$4 \cdot 10^{-4}$
4	60	10	0.17	46.79	$7.8 \cdot 10^{-4}$
5	100	15	0.15	23.88	$2.4 \cdot 10^{-4}$
6	160	0	0	23.88	$1.5 \cdot 10^{-4}$
7	160	5	0.03	0.21	$1.3 \cdot 10^{-6}$
8	160	5	0.03	2.88	$1.8 \cdot 10^{-5}$
9	160	5	0.03	23.88	$1.5 \cdot 10^{-4}$
10	160	15	0.09	46.79	$2.9 \cdot 10^{-4}$
11	160	20	0.13	23.88	$1.5 \cdot 10^{-4}$
12	160	25	0.16	0.86	$5.4 \cdot 10^{-6}$
13	160	25	0.16	23.88	$1.5 \cdot 10^{-4}$
14	160	25	0.16	46.79	$2.9 \cdot 10^{-4}$
15	160	40	0.25	23.88	$1.5 \cdot 10^{-4}$
16	160	Circular		0.21	$1.3 \cdot 10^{-6}$
17	160	Circular		2.88	$1.8 \cdot 10^{-5}$
18	160	Circular		23.88	$1.5 \cdot 10^{-4}$
19	160	Circular		46.79	$2.9 \cdot 10^{-4}$
20	250	25	0.1	23.88	$1.0 \cdot 10^{-4}$
21	400	20	0.05	0.21	$5.3 \cdot 10^{-7}$
22	400	20	0.05	2.88	$7.2 \cdot 10^{-6}$
23	400	20	0.05	23.88	$6.0 \cdot 10^{-5}$
24	400	20	0.05	46.79	$1.2 \cdot 10^{-4}$
25	400	40	0.1	23.88	$6.0 \cdot 10^{-5}$
26	170	Circular (wood)		2.8	$1.6 \cdot 10^{-5}$
27	170	Circular (real)		1.92	$1.1 \cdot 10^{-5}$

3.4 The end plates

When testing in a wind tunnel, the model has a finite length and the model extremities and side walls could introduce secondary effects [27,28]. Slaouti and Gerrard [29] demonstrated that these effects have a strong influence on the near wake and then on the drag coefficient. To guarantee the bidimensionality of the flow around the cylinder, end plates are added perpendicularly to the cylinder axis. This is the reason for using the rectangular insert described just before.

At high Reynolds numbers, the cylinder aspect ratio should be higher than 3 times the model diameter [30, 31]. In our experiments, the end plates are separated by 1.3 m, leading to aspect ratios ranging from 3.25 to 22.

The end plates need also to be very large [32]. Their size influences strongly the length over which the flow can be considered as bidimensional. In our experiments, the ratio between the total length of the end plates (upstream and downstream the model) and the diameter of the cylinder ranges from 10 to 26 depending on the cylinder diameter. Finally, if the upstream or the downstream length of the end plates is too small, secondary effects could influence the upstream flow or the wake. In the present case, the length of the end plates downstream the model is equal to 1.75 m, which is higher than the value of 4.25 x d suggested by Kubo et al. [33]. The upstream length of the end plates is equal to 2.5 m, which proved to be sufficient since a reference plane with uniform pressure distribution (static and dynamic) has been identified at 1.8 m upstream of the model.

3.5 Blockage effect

The measurement of drag coefficient requires the use of very large wind tunnels, like the VKI L1-A wind tunnel, in order to limit the wall effects on the measured results. Wall effects are present for both open and closed wind tunnels and referred to as blockage effect. In practice, one can neglect blockage effect when the wind tunnel cross-section is at least 30 times larger than the model cross-section (blockage ratio smaller than 3%) [34].

However, the present investigation is considering models associated to blockage ratios up to 17%. Blockage corrections are then necessary. A comparison between closed and open test sections in the case of normal flat plates and rectangular blocks, both centrally-mounted in the test section, showed that the closed test section overestimates the drag coefficient while the open test section shows a drag reduction [35]. The blockage effect in the open test section is less than in the closed one. However, as indicated in the AGARDograph 336 on "Wind Tunnel Wall Correction" [35], it is more suitable to perform measurements in a closed test section since the correction formulations are better developed and the boundaries are more precisely defined in this case. The corrected drag coefficients obtained from a closed test section are certainly more reliable than those measured in an open test section without correction [35].

Formulations for blockage correction exist in the literature for flap plates and circular cylinders at low or high Reynolds numbers [36-41]. However, none of these correction models is valid for all the flow regimes, as shown by Anthoine et al. [36]. To optimize the correction and reduce the scatter of the results, different correction models should be combined depending on the flow regimes. Such a combined procedure for correcting the blockage effect has been applied at VKI to three smooth circular cylinders in similitude and validated for all the flow regimes against literature data [36]. Since the database (Table 2) do not include octagonal cylinders in geometrical similitude (including edge radius and surface roughness), it was not possible to validate the blockage correction procedure for these cylinders. However, the uncertainty due to the blockage correction has been estimated.

3.6 The measurement uncertainty

The global uncertainty of the measurements takes into account the uncertainty due to the blockage correction and the uncertainty on the test conditions. The last one includes the instrumentation error, the effect of the test section and of the model positioning, among others.

3.6.1 Circular cylinders

As indicated above, a procedure for blockage correction has been applied successfully to circular cylinders for blockage ratio ranging from 6,8% to 17% [36]. The scattering observed in the raw data (before correction) of drag coefficient has been reduced significantly and the resulting corrected drag coefficients are validated by the literature data. So, there is no uncertainty associated to the blockage correction.

The only uncertainty is due to the test conditions. Table 3 provides the global uncertainty for the circular cylinders depending on the flow regime.

Table 3 – Global uncertainty – circular cylinders

Sub-critical flow regime	Critical flow regime	Super-critical flow regime
8%	14%	2%

3.6.2 Octagonal cylinders

There is no formulation for blockage correction available and validated for octagonal cylinders. All the data acquired during this investigation are then corrected using the formulation of Allen and Vincenti [38]. This correction overestimates the real drag by a maximum value equal to the uncertainty due to the blockage error. Therefore, no uncertainty will be added to this correction. Since the acquired data will be used during the design phase of the lighting columns, keeping overestimated values remains a better choice than using real ones associated to an uncertainty.

The only uncertainty is due to the test conditions. Tables 4 and 5 provide the global uncertainty for the octagonal cylinders depending on the Reynolds number for the cylinders without transition and depending on the flow regime for the cylinders with transition.

Table 4 – Global uncertainty – circular cylinders without transition

Low Reynolds (< 200000)	High Reynolds
9 %	4 %

Table 5 – Global uncertainty – circular cylinders with transition

Sub-critical flow regime	Critical flow regime	Super-critical flow regime
9%	11%	2%

4 Results

4.1 Influence of the surface roughness

The influence of the surface roughness on the drag coefficient of circular cylinders is summarized in Fig. 3 and Table 6. At low Reynolds number, the drag coefficient is independent of the roughness. Moreover, there is a minimum roughness (of the order of 2×10^{-5}) below which the evolution of the drag coefficient is not influenced by the surface roughness. On the other hand, the transition appears for smaller Reynolds number when the roughness increases. In such condition, the drag coefficient in the high Reynolds number range can be multiplied up to a factor of 3 compared to the smooth circular cylinder ($C_D = 0.9$ in place of $C_D = 0.3$).

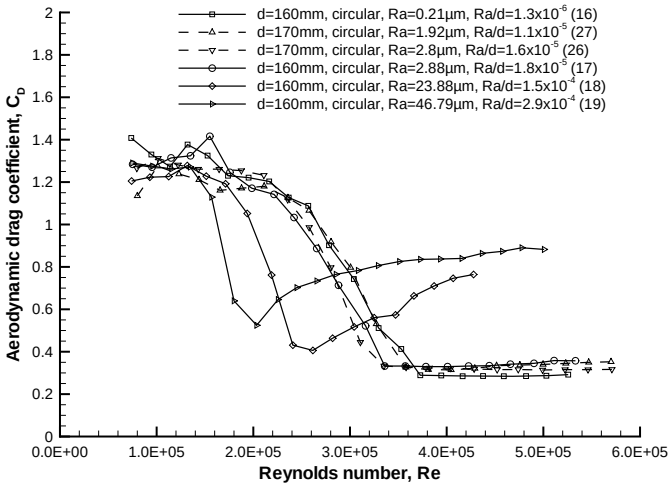

Fig. 3 – Influence of the surface roughness for circular cylinders

Table 6 – Influence of the surface roughness – circular cylinders

Ra/d	Re < 1.5×10^5	Re_{min}	$C_{D,min}$	Re > 5×10^5
1.3×10^{-6}	1.25	3.7×10^5	0.30	0.30
1.8×10^{-5}	1.25	3.4×10^5	0.33	0.35
1.5×10^{-4}	1.25	2.5×10^5	0.40	0.75
2.9×10^{-4}	1.25	1.9×10^5	0.50	0.90

Fig. 4 and 5, as well as Tables 7 and 8, show the influence of the surface roughness for octagonal cylinders with sharp edges and rounded edges, respectively. As for the circular cylinders, the roughness has no effect on the drag coefficient at low Reynolds number. For higher Reynolds number values, an increase of the roughness leads on one side to a reduction of the drag coefficient for the cylinders with sharp edges, but on the other side to a rise of the drag coefficient for the cylinders with rounded edges. The influence of the roughness is then highly dependent on the cross-section shape and on the edge radius.

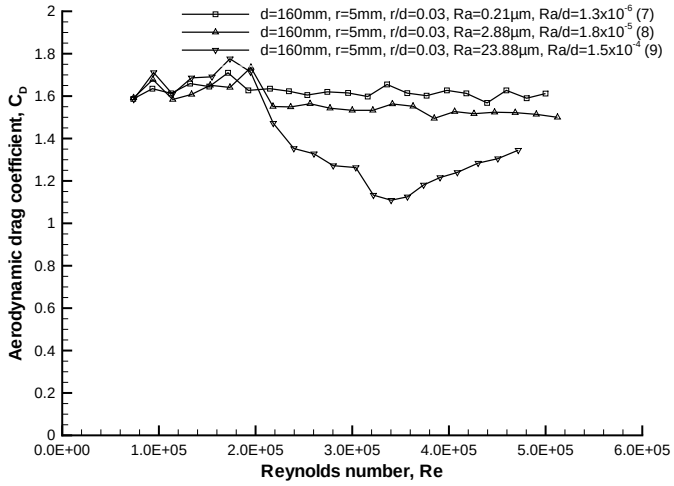

Fig. 4 – Influence of the surface roughness for octagonal cylinders with sharp edges

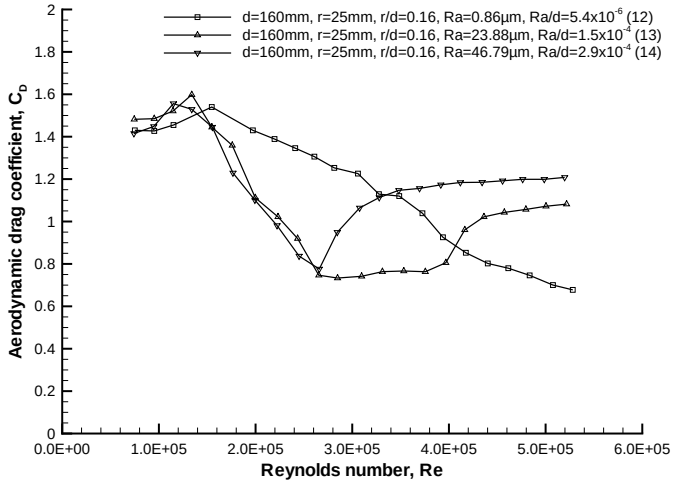

Fig. 5 – Influence of the surface roughness for octagonal cylinders with rounded edges

Table 7 – Influence of the surface roughness – octagonal cylinders with sharp edges (r/d = 0.03)

Ra/d	Re < 1.5×10^5	Re_{min}	$C_{D,min}$	Re > 5×10^5
1.3×10^{-6}	1.65	--	--	1.6
1.8×10^{-5}	1.6	--	--	1.5
1.5×10^{-4}	1.7	3.3×10^5	1.1	1.3

Table 8 – Influence of the surface roughness – octagonal cylinders with rounded edges (r/d = 0.156)

Ra/d	Re < 1.5×10^5	Re_{min}	$C_{D,min}$	Re > 5×10^5
5.4×10^{-6}	1.5	$> 6\ 10^5$	--	0.7
1.5×10^{-4}	1.45	$2.6\ 10^5 – 4\ 10^5$	0.75	1.1
2.9×10^{-4}	1.5	$2.6\ 10^5$	0.8	1.2

4.2 Influence of the edge radius

As shown in Fig. 6 and Table 9, a smooth octagonal cylinder with sharp edges behaves like a bluff body, meaning that the drag coefficient remains independent of the Reynolds number. For low roughness values, a transition appears when the edge radius increases. When the edge radius is higher, the cylinder behaves closer to a smooth circular cylinder.

For larger values of the surface roughness (Fig. 7 and Table 10), the transition is always present whatever the edge radius. An increase of that radius reinforces the transition. At the limit (for high edge radius), the cylinder behaves again like a circular cylinder.

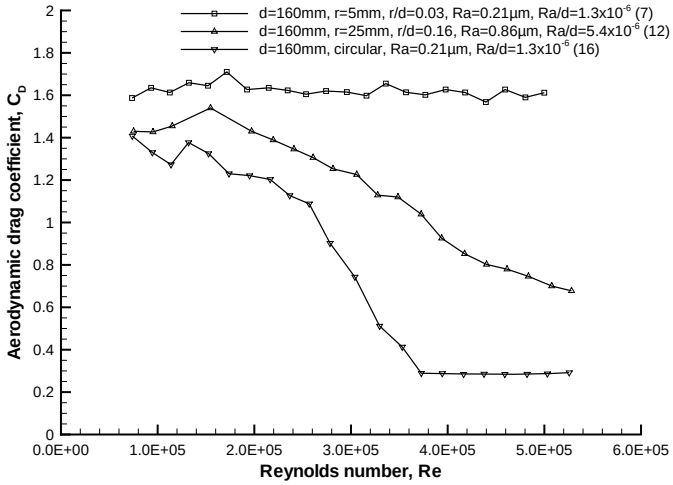

Fig. 6 – Influence of the cross-section shape – smooth cylinders

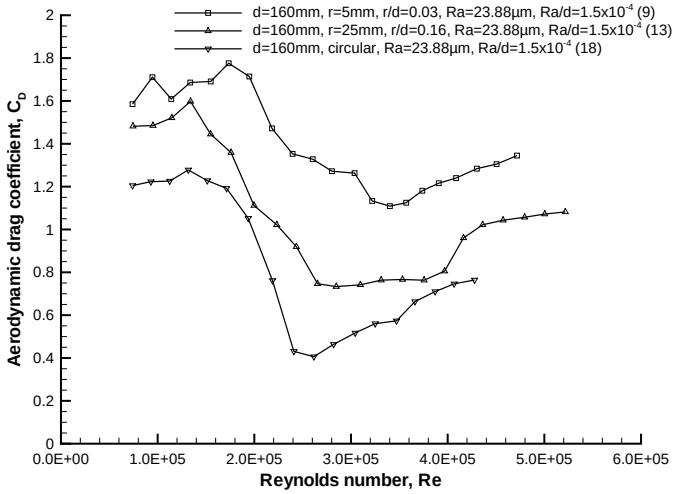

Fig. 7 – Influence of the cross-section shape – rough cylinders

Table 9 – Influence of the cross-section shape – smooth cylinders ($Ra/d < 10^{-5}$)

Cross-section	Re < 1.5×10^5	Re_{min}	$C_{D,min}$	Re > 5×10^5
Octagonal (r/d = 0.03)	1.65	--	--	1.6
Octagonal (r/d = 0.16)	1.5	$> 6\ 10^5$	--	0.7
Circular	1.25	3.7×10^5	0.30	0.30

Table 10 – Influence of the cross-section shape – rough cylinders ($Ra/d = 1.5 \times 10^{-4}$)

Cross-section	Re < 1.5×10^5	Re_{min}	$C_{D,min}$	Re > 5×10^5
Octagonal (r/d = 0.03)	1.7	3.3×10^5	1.1	1.3
Octagonal (r/d = 0.16)	1.45	2.6×10^5 – 4×10^5	0.75	1.1
Circular	1.25	$2.5\ 10^5$	0.40	0.75

Generally, whatever the Reynolds number, an increase of the edge radius reduces the drag coefficient, as indicated in Fig. 8 and Table 11.

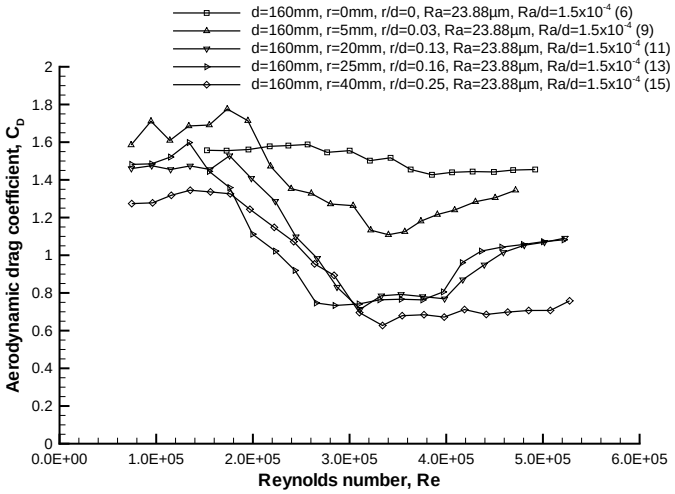

Fig. 8 – Influence of the edge radius

Table 10 – Influence of the edge radius ($Ra/d = 1.5 \times 10^{-4}$)

r/d	Re < 1.5×10^5	Re_{min}	$C_{D,min}$	Re > 5×10^5
0	1.65	--	--	1.5
0.03	1.7	3.3×10^5	1.1	1.3
0.13	1.45	3.1×10^5 – 4×10^5	0.75	1.1
0.16	1.45	2.6×10^5 – 4×10^5	0.75	1.1
0.25	1.3	3.3×10^5 – 5.1×10^5	0.65	--

4.3 Influence of the wind angle of attack

All the previous tests (Table 2) have been acquired with a side of the model oriented towards the wind direction to comply with the standard in force. However, the wind direction can change in the real situation and it is then necessary to determine the sensitivity of the drag coefficient to the wind angle of attack.

When the octagonal cylinder is oriented in such a way that the flow is not anymore symmetrical compared to the flow direction, then a lateral force is added to the drag force. The amplitude of this force is more or less important depending on the wind angle of attack and the resulting total force is not anymore equal to the drag force.

Two octagonal cylinders have been considered to assess the influence of the flow direction: model 7 (160 mm, smooth and sharp edges) and model 13 (160 mm, rough and rounded edges). These cylinders are representative of the two extreme kinds of drag evolution. Indeed, model 7 corresponds to a bluff body without transition (Fig. 4), while model 13 shows an important transition with a "plateau" of minimum C_D value (Fig. 5).

Measurements are carried out for angles of attack between 0° (side oriented towards the wind) and 22.5° (ridge oriented towards the wind).

The maximum force coefficient to consider for the design of an octagonal lighting is the total force coefficient. The wind angle of attack corresponding to the maximum value of this total coefficient varies with the geometry of the model (through the transition) and with the Reynolds number, as indicated in Table 11.

For a smooth octagonal lighting column without transition, one should use the total force coefficient C_T at 0° (or the drag force C_D at 0° as first approximation since the lateral force is negligible at 0°), as indicated in Fig. 9. For the other cases (with transition), one should combine the total force coefficient C_T at 0° at low Reynolds number (Re < 200000) and the coefficient C_T at 20° at high Reynolds number, as shown in Fig. 10.

Table 11 – Force coefficient to use for the design of octagonal lighting column

	Re < 2×10^5	Re > 2×10^5
Smooth – Sharp edges	C_T at 0°	C_T at 0°
Smooth – Rounded edges	C_T at 0°	C_T at 20°
Rough – Sharp edges		
Rough – Rounded edges		

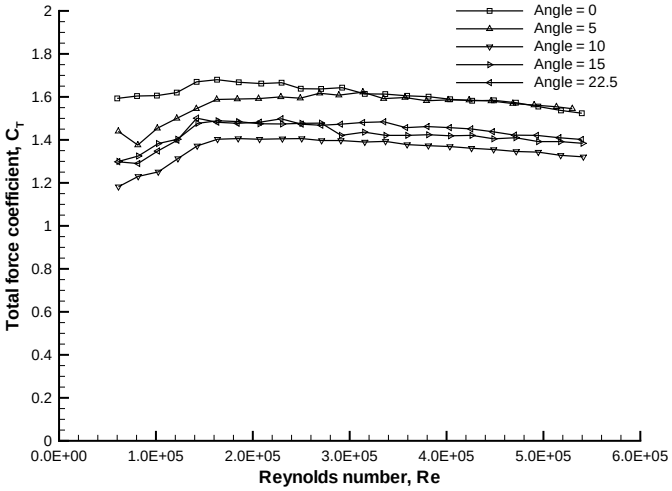

Fig. 9 – Model 7 – Influence of the wind angle of attack

For all the models without transition, it is possible to make the design based on the test results obtained at 0°. However, it is not possible to generalize this conclusion

to the other models with transition. Since the database presented in Table 2 has been obtained for a wind angle of attack of 0°, the aerodynamic force coefficient needed for the design is available only at low Reynolds number but not at high Reynolds number. To get this coefficient for the other models presenting a transition, which needs to be measured with 20° of wind angle of attack, a complementary test campaign is planned.

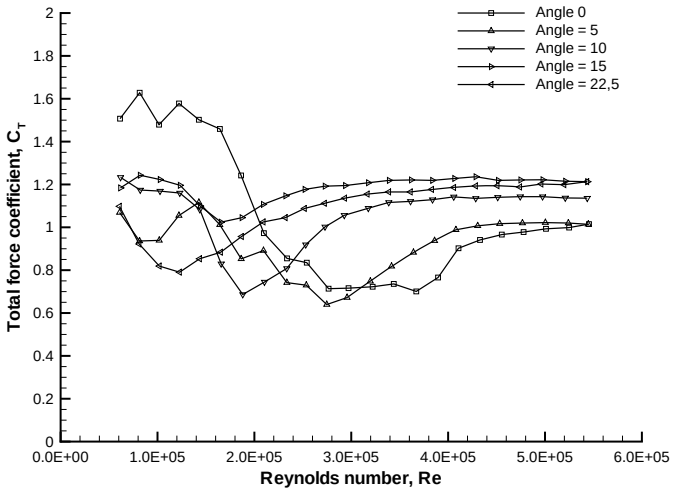

Fig. 10 – Model 13 – Influence of the wind angle of attack

5 Concluding remarks

The present paper described the experimental database available for the determination of the aerodynamic force coefficient of public lighting columns. This database showed that the force coefficients for octagonal cylinders depend strongly on the surface roughness and rounded edge radius. They are also more important than for the circular cylinders, especially at high Reynolds number. However, a complementary test campaign is needed for the octagonal cylinders with transition (most critical for rough surface and rounded edges) to provide the total force coefficient under 20° of wind angle of attack, since it has been proved that this value is the most restricting at high Reynolds number (Re > 200000).

References:

[1] Houghton, E.L. and Carpenter, P.W., *Aerodynamics for engineering students*, Butterworth & Heinemann, Fifth Edition, 2003.

[2] Zdravkovich, M.M., *Flow around circular cylinders, Vol. 1: Fundamentals*, Oxford science publications, 1997.

[3] Zdravkovich, M.M., *Flow around circular cylinders, Vol. 2: Applications*, Oxford science publications, 2003.

[4] Roshko, A., Experiments on the flow past a circular cylinder at very high Reynolds numbers, *J. Fluid Mech.*, Vol. 10, pp, 345-356, 1961.

[5] Lakehal, D., Computation of turbulent shear flows over rough-walled circular cylinders, *J. of Wind Engineering and Industrial Applications*, Vol. 80, pp. 47-68, 1999.

[6] Hoerner, S., *Fluid dynamic drag*, published by the author, 1958.

[7] Batchelor, G.K., *An introduction to Fluid Dynamics*, Cambridge University Press, 2001.

[8] Roshko, A, Fiszdon, W., Of the persistence of transition in the near-wake, *Problem in Hydrodynamics and Continuum Mechanics, Philadelphia*, SIAM, pp.606-616, 1969.

[9] Anderson, J.D., *Fundamental Aerodynamics*, Mc Graw Hill, 2002.

[10] British standard institution, code of basic, data for the design of buildings, CP. 3, chapter 5: Loading.

[11] Achenbach, E., "Influence of surface roughness on the cross-flow around a circular cylinder", J. Fluid Mech., Vol. 46(2), pp. 321-335, 1971.

[12] Ribeiro, J., "Effects of surface roughness on the two-dimensional flow past circular cylinders – I: mean forces and pressures, J. of Wind Engineering and Industrial Applications, Vol. 37, pp. 299-309, 1991.

[13] Adachi, T., "Effects of surface roughness on the universal Strouhal number over the wide Reynolds number range", J. of Wind Engineering and Industrial Applications, Vol. 69-71, pp. 399-412, 1997.

[14] Farell, C. and Fedeniuk, S.K., "Effect of end plates on the flow around rough cylinders", 7th International Conference on Wind Engineering, Aachen, West Germany, July 6-10, 1987, Vol. 2, pp. 87-98.

[15] Guven, O., Patel, V.C. and Farell, C., "Surface roughness effects on the mean flow past circular cylinders", Iowa institute of Hydraulic Research, Report No. 175, 1975.

[16] Buresti, G., "The effect of surface roughness on the flow regime around circular cylinders", J. of Wind Engineering and Industrial Applications, Vol. 8, pp. 105-114, 1981.

[17] Williamson, C.H.K., "Vortex dynamics in the cylinder wake", Ann. Rev. Fluid. Mech., pp. 477-627, 1996.

[18] Tamura, T. and Miyagi, T., "The effect of turbulence on aerodynamic forces on a square cylinder with various corner shapes", J. of Wind Engineering and Industrial Applications, Vol. 83, pp. 135-145, 1999.

[19] So, R.M.C. and Savkar, S.D., "Buffeting forces on rigid circular cylinders in cross flows", J. Fluid Mech., Vol. 105, pp. 397-425, 1981.
[20] Cheung, J.C.K. and Melbourne, W.H., "Turbulence effects on some aerodynamic parameters of a circular cylinder at supercritical Reynolds numbers", J. of Wing Eng. and Ind. Aerodynamics, Vol. 14, pp.399-410, 1983.
[21] Szalay, Z., "Drags on several polygon cylinders", 7th International Conference on Wind Engineering, Aachen, West Germany, July 6-10, 1987, Vol. 4, pp. 21-30.
[22] "Eurocode for lighting columns wind loading, assessment of EN40: part 60", second draft, Flint and Neill Partnership, London, March 1993.
[23] ESDU Data Item 79026, "Mean fluid forces and moments on cylindrical structures: polygonal sections with rounded corners including elliptical shapes", Oct. 1979.
[24] Bearman, P.W. and Trueman, D.M., "An investigation of the flow around rectangular cylinders", Aeronautical Quarterly, Vol. 23, pp. 229-237, 1972.
[25] Tamura, T. and Kuwahara, K., "Numerical study of aerodynamic behavior of a square cylinder", J. of Wind Engineering and Industrial Applications, Vol. 33, pp. 161-170, 1990.
[26] Cowdrey, C.F. and Lawes, J.A., "Force measurements on square and dodecagonal sectional cylinders at high Reynolds numbers", National Physical Laboratory, NPL/Aero/351, 1959.
[27] Fox, K.A. and West, G.S., "On the use of end plates with circular cylinders", Experiments in Fluids, Vol. 9, pp. 237-239, 1990.
[28] Norberg, C., "An experimental investigation of the flow around a circular cylinder: influence of aspect ratio", J. Fluid Mech., Vol. 258, pp. 287-316, 1994.
[29] Slaouti, A. and Gerrard, J.H., "An experimental investigation of the end effects on the wake of a circular cylinder towed through water at low Reynolds numbers", J. Fluid Mech., Vol. 112, pp. 297-314, 1981.
[30] Chen, P.Y. and Doepker, P.E., "Flow-induced forces on a cylinder for different wall confinements at high Reynolds numbers (3.5·105) < Re < (3.5·106)", Transactions of ASME, Journal of Pressure Vessel Technology, May 1975, pp. 110-117.
[31] Achenbach, E., "Distribution of local pressure and skin friction around a circular cylinder in cross flow up to R = 5 x 106", J. Fluid Mech., Vol. 34, 1968, p. 625.
[32] Stansby, P.K., "The effects of end plates on the base pressure coefficient of a circular cylinder", Aeronautical Journal, Vol. 78, pp.36-37, 1983.
[33] Kubo, Y., Miyazaki, M., Kato, K., "Effects of end plates and blockage of structural members on drag force", J. of Wing Eng. and Ind. Aerodynamics, Vol. 32, pp.329-342, 1989.
[34] Barlow, J.B., Rae, W.H, Pope, A., "Low speed wind tunnel testing", 3rd edition, John Wiley & Sons Inc., 1999.
[35] Cooper K.R., "Bluff-body blockage corrections in closed and open test section wind tunnels" in AGARD-AG-336 "Wind tunnel wall corrections", Chapter 6, pp. 1-33,NATO, 1998.
[36] Anthoine, J., Olivari, D., Porgugaels, D., Drag coefficient determination of bluff bodies – analysis of blockage effect, COST Action C14, Impact of Wind and Storm on City life and Built Environment, Rhode Saint Genèse, Belgium, May 5-7, 2004.
[37] Lock, C.N.H., "The interference of a Wind Tunnel on a Symmetric body", British ARC, R&M 1275, 1929.
[38] Allen, H.J. and Vincenti, W.G., "Wall Interference in a Two-Dimensional Flow Wind Tunnel, with Consideration for the Effect of Compressibility", NACA Technical Report No. 782, 1944.
[39] Fage, A., "On the Two Dimensional Flow Past a Body of symmetrical Cross-section Mounted in a Channel of finite Breadth", British ARC, R&M 1233, 1929.
[40] Maskell, E.C., "A theory of the blockage effects on bluff bodies and stalled wings in a closed wind tunnel", RAE Report AERO 2685, November 1963.
[41] Hackett, J.E., Cooper, K.R., "Extensions to Maskell's theory for blockage effects on bluff bodies in a closed wind tunnel", Aeronautical J., Vol. 105, 2001, pp.409-418.